UNDERSTANDING OF HYDRIDING MECHANISMS OF ZIRCALOY-4 ALLOY DURING CORROSION IN PWR SIMULATED CONDITIONS AND INFLUENCE OF ZIRCONIUM HYDRIDES ON ZIRCALOY-4 CORROSION

C. BISOR-MELLOUL, M. TUPIN, P. BOSSIS
DEN/DANS/DMN/SEMI, CEA
CEA/Saclay, 91191 Gif-sur-Yvette – France

J. CHENE
DEN/DANS/DPC/SCCME, CEA
CEA/Saclay, 91191 Gif-sur-Yvette – France

J. L. BECHADE
DEN/DANS/DMN/SRMA, CEA
CEA/Saclay, 91191 Gif-sur-Yvette – France

A. MOTTA
Mechanical and Nuclear Engineering Department, Penn State University
227 Reber Building, University Park, PA 16802 – USA

ABSTRACT

Zirconium alloys are widely used as fuel claddings in Power Water Reactors. As they represent the first containment barrier to fission products, their mechanical integrity is essential for nuclear safety. During their corrosion in primary water, some of the hydrogen involved in the oxidation reaction with water ingresses into the alloy through the oxide layer. In the metallic matrix, once the solid solution limit is reached at the irradiation temperature, hydrogen precipitates as Zr hydrides mainly located just under the metal/oxide interface due to the thermal gradient across the cladding. As these hydrides may contribute to a larger oxide thickness and to a more fragile behaviour of the cladding, the minimization of hydrogen pick-up is required. Accordingly, since the Zircaloy-4 (Zr-1.3Sn-0.2Fe-0.1Cr) alloy is known to be sensitive to this phenomenon, the understanding of its hydriding mechanism and of the influence of zirconium hydrides on its corrosion behaviour is needed. Regarding the study of the hydriding mechanism, isotopic exchanges were carried out in D_2O environment at 360°C and led to the localization, in the oxide scales, of the limiting step for the hydrogen diffusion. To estimate an apparent diffusion coefficient of hydrogen in the oxide formed on Zircaloy-4, we firstly based on SIMS profiles and penetration depth of deuterium in the dense part of the oxide film. Secondly, ERDA estimation of the hydrogen content in zirconia and fusion measurements of the hydrogen content in both metal and oxide were used to estimate a hydrogen flux absorbed by the alloy and hence to deduce an apparent diffusion coefficient. Finally, these two methods lead to quite similar values (between 2.10^{-14} cm²/s and 6.10^{-14} cm²/s) which are in accordance with bibliography. Concerning the impact of hydrides on the corrosion of Zircaloy-4, several pre-hydrided and reference samples were corroded simultaneously in primary water at 360°C. The characterization of the pre-hydrided samples revealed some changes compared with the reference ones, such as the presence of the Zr_3O sub-oxide at the inner metal/oxide interface, a lower fraction of β-ZrO_2 in the oxide and a faster diffusion of oxygen species through grain boundaries of zirconia (TEM, µ-XRD, ^{18}O isotopic experiments). Moreover, during oxidation, the hydrogen initially present in the hydride phase remains in the metallic matrix and leads to the allotropic transformation δ–$ZrH_{1,66}$ → ε–ZrH_2.

1 Introduction

In Pressurized Water Reactors, zirconium alloys used as fuel claddings are exposed to aggressive aqueous environment (285-325℃, 155 bars , 0.7 to 2.2 ppm Li and 10 to 1200 ppm B). In these conditions, the corrosion kinetics of Zircaloy-4 (Zr-1.3Sn-0.2Fe-0.1Cr) shows a drastic acceleration phase referred as “phase III” which occurs for fuel burnups above 40 GWd/tU [1]. To explain this acceleration, three major hypotheses were proposed by authors. The first advanced cause could be the tin content in the alloy [1] [2] [3]. A second assumption assigned the accelerated corrosion to the impact of the dissolution of $Zr(Fe,Cr)_2$ precipitates under irradiation [4] [5], whereas, several authors suggested that this enhanced corrosion rate would be rather due to the precipitation of massive hydrides at the metal/oxide interface, in the metallic part of the cladding [6] [7] [8] [9]. Indeed, during their corrosion in primary water, some of the hydrogen involved in the reaction with water ingresses into the alloy through the oxide film and finally precipitates as Zr hydrides heterogeously located in the underlying metal, just beneath the metal/oxide interface. Many studies tried to understand the nature of the link between the precipitation of massive hydrides in the cladding and its further oxidation rate [6] [7] [8] [9] [10] [11]. However, the extent of the impact of a hydride rim under the metal/oxide interface on the corrosion kinetics is still under debate. In relation with these investigations, several studies tried to determine the hydriding mechanisms through the oxide scale [12] [13] [14] [15] [16] in order to explain the hydrogen pick-up fraction (HPUF) of the Zircaloy-4 cladding, which is between 15% and 20% in PWRs [17].
Presently, nuclear operators wish to enhance fuel burnups up to 60 GWd/tU, and the corrosion and hydriding of Zircaloy-4 claddings have become the limiting factor in the lifetime of the fuel assembly made of this alloy. In this purpose, the understanding of the hydriding mechanisms of the alloy and the impact of hydrides on its corrosion behaviour is required.

2 Understanding of hydriding mechanisms of Zircaloy-4

2.1 Experimental procedures and techniques

The Zircaloy-4 samples were corroded in static autoclaves at 360℃ and 18.7 MPa in light primary water (H_2O, 2 ppm Li, 1000 ppm B). To understand the hydriding mechanisms of these samples, isotopic exchanges of hydrogen were carried out. In a first step, all the samples were corroded with specific times of exposure in order to obtain oxide thicknesses in the pre or in the post transition phase of Zircaloy-4 oxidation kinetics. Then, in a second step, the specimens were corroded in heavy primary water during short or long time exposures, in order to investigate the hydriding mechanisms of the alloy. In parallel, some samples were used to follow the corrosion kinetic behaviour of the alloy. After exposure, some fusion measurements were carried out to estimate the hydrogen uptake of the samples. The experimental procedure and techniques have been detailed in a previous article [18].

2.2 Corrosion tests results

The corrosion behaviour at 360℃ in PWR conditions of Zircaloy-4 was measured: the kinetic curves of two samples are presented in figure 1. According to literature data, it is well known that the pre-transition stage of Zircaloy-4 corrosion is characterized by the growth of a dense and protective oxide layer via a diffusion process of oxygen vacancies [19]. The kinetic curve of this oxidation follows a sub-parabolic law shaped as $x = kt^n$ with an n parameter included between 0.3 and 0.5 [20]. The experimental points on both samples are reproducible and were fitted according to the following law (dotted line):

$$x = 0.47.t^{0.3} \qquad \text{(eq. 1)}$$

with x representing the oxide thickness (µm) and t the corrosion duration (days).

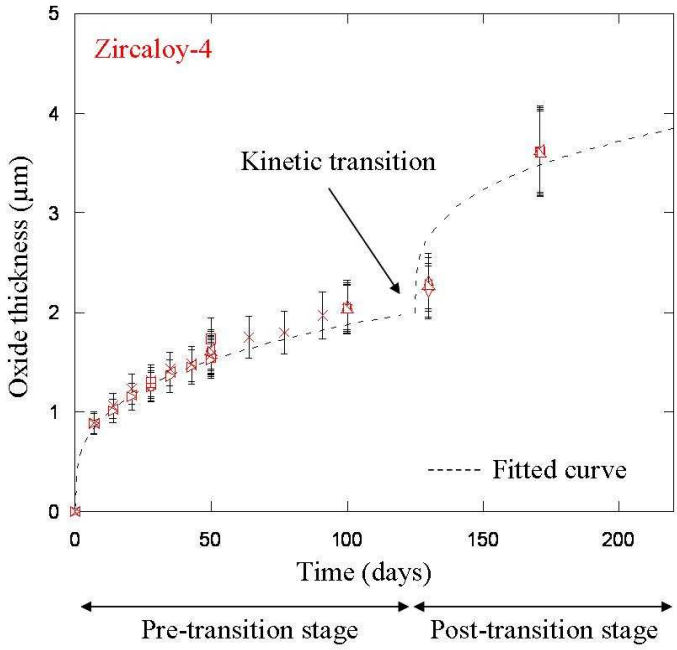

Fig. 1. Corrosion kinetics of Zircaloy-4 samples during corrosion in primary water at 360℃ and 18.7 MPa. The kinetic transition appears around 2 µm and 125 days of corrosion.

When the alloy reaches the kinetic transition, around 2 µm, the oxide cracks [21] [22] and becomes porous [23] [24] [25] whereas a new protective film is forming at the interface. Hence, in the post-transition stage, the oxide is divided into two sub-layers: the external one, which presents a lot of defects as pores and cracks, and a quite dense internal layer near the metal/oxide interface. In this post-transition region, a new corrosion cycle occurs and can be fitted with the same previous law (eq. 1).

The hydrogen contents absorbed by the alloy during corrosion were determined, before and after the kinetic transition. The results seem to be in agreement with bibliography with an average hydrogen pick-up fraction of 12%.

2.3 Estimation of the apparent diffusion coefficient of hydrogen in the oxide scale at 360℃

After the corrosion tests, the samples were analyzed using SIMS technique. The hydrogen profile obtained after 50 days of corrosion in light primary water in the pre-transition stage is shown in figure 2. As seen in this figure, the pre-transition oxide is divided into two sub-layers, regarding the hydrogen content: an external one whose thickness is around 300 nm, and an internal one, with a thickness close to 1.3 µm. In literature, the same sub-division is reported and associated with the microstructure of the oxide scale. In particular, the outer layer is permeable to hydrogen whereas the inner part of the film is dense [12] [26]. These results were confirmed with a re-oxidation of the sample in heavy primary water during a long exposure.
In the other side of the interface (fig. 2a), in the metallic part, the hydrogen profile indicates a high heterogeneous content which is linked to the hydrogen absorbed during the corrosion process. After the cooling, at the ambient temperature, the hydrogen solubility is very low [27] and its precipitation leads to the formation of zirconium hydrides. The crater image obtained after the abrasion of the sample by the ion beam is presented in figure 2b and highlights the over-concentrated hydrogen zones in the metal.

To estimate the apparent diffusion coefficient of hydrogen in the dense (internal) part of the oxide, the same sample was re-oxidized in heavy primary water during a short exposure so that the isotope did not reach the metal/oxide interface. Indeed, entering a bulk diffusion coefficient and a grain boundary diffusion coefficient in the Cast3m code ($D_b = D_{gb} = D_a$), we tried to describe the experimental curve obtained after the 6 hour-exposure in D_2O. An estimation of D_a can be made between 2.10^{-14} cm²/s and 6.10^{-14} cm²/s, and we showed that it can be considered as equal for the dense part of the pre-transition and the post-transition oxide films.

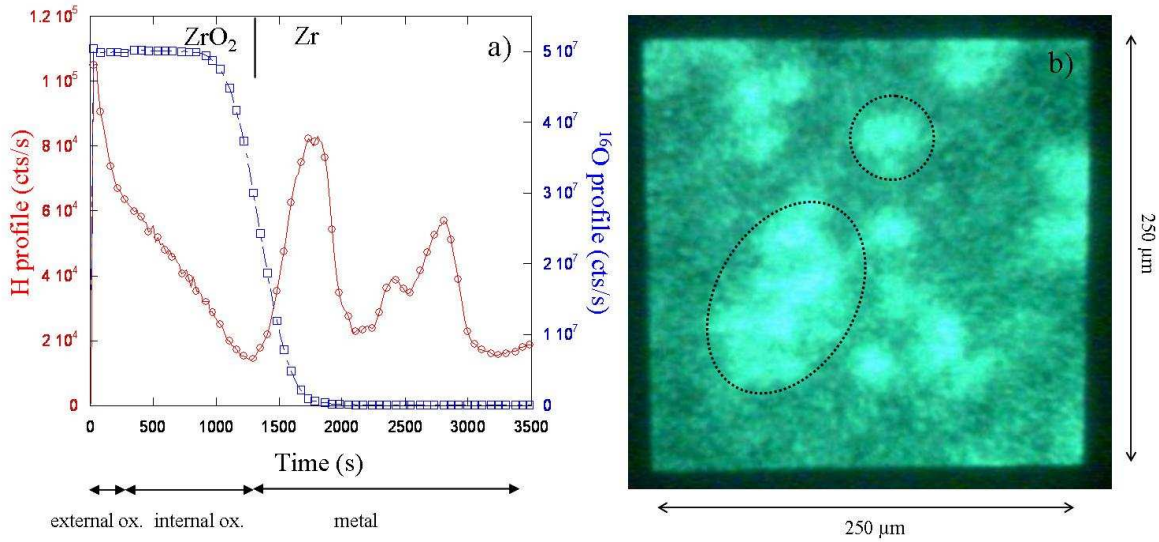

Fig. 2. a) SIMS profiles of hydrogen and oxygen obtained after a 50 day-corrosion in PWR conditions of a Zircaloy-4 sample in the pre-transition region. b) Corresponding image of the crater after the SIMS analysis. Bright zones correspond to the high level contents of hydrogen in the metallic part of the alloy.

In complement of SIMS analyses, the Elastic Recoil Detection Analysis (ERDA) technique can be used to quantify the hydrogen contents obtained in the pre-transition and in the post-transition oxides and to estimate, via another way of calculation, the apparent diffusion coefficient of hydrogen in the dense part of the corrosion films formed on Zircaloy-4 alloy. The figure 3 presents the scanning electron micrograph of the post-transition sample (tapered cross-section with a bias angle of 10°) co upled with the corresponding hydrogen cartography obtained by ERDA. Based on these data and on the hydrogen content obtained by fusion measurements, the expression of the hydrogen flux (in steady state) absorbed by the alloy during the time of corrosion can be integrated and D_a can be deduced. A more precise demonstration has been proposed in another article [18]. Finally, at 360°C, the apparent diffusion coefficient of hydrogen deduced from the ERDA results in the pre-transition and in the post-transition oxides are in good agreement with the estimation based on the SIMS / CAST3M experiment. These values are similar and validate the hypothesis of a same apparent diffusion coefficient of hydrogen in the oxide, no matter if the kinetic transition is reached or not. Based on these results, an average value of 2.10^{-14} cm²/s can be proposed for the apparent diffusion coefficient of hydrogen in oxides grown on Zircaloy-4.

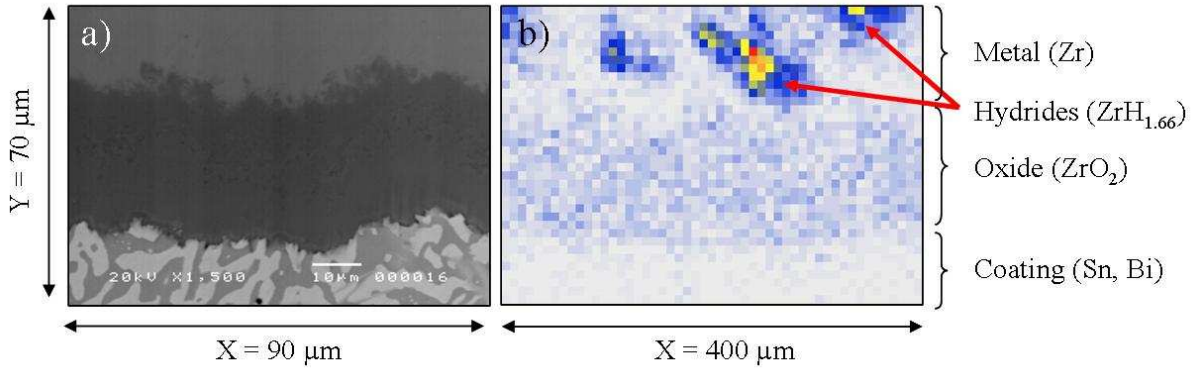

Fig. 3. a) Scanning electron micrograph of a tapered cross-section of the post-transition oxide. b) Corresponding hydrogen cartography obtained by ERDA. Heterogeneous hydrogen distribution in the metallic part of the sample can be associated with the figure 2b and the presence of zirconium hydrides.

3 Impact of zirconium hydrides on Zircaloy-4 corrosion in primary water

3.1 Experimental procedures and techniques

To estimate the impact of zirconium hydrides on Zircaloy-4 corrosion, several samples were cathodically charged with hydrogen in order to precipitate a dense δ-$ZrH_{1.66}$ phase on the outer surface, which is called “rim”, of the specimens. The hydriding protocol was similar to the one qualified by EDF R&D laboratory [8]. In a second step, these samples were corroded simultaneously with reference un-hydrided samples in light primary water at 360℃ in order to compare their oxidation kinetics, their oxide microstructure, and the diffusion of oxygen in the oxide film (through isotopic exchange with ^{18}O). All the experimental procedures and techniques have been detailed elsewhere [28].

3.2 Impact of zirconium hydrides on oxidation kinetics of Zircaloy-4

The corrosion behaviour at 360℃ in PWR conditions of pre-hydrided Zircaloy-4 samples were analyzed and compared with reference specimens (fig. 4). For each group of specimens, the reproducibility of kinetic curves is quite satisfactory and an impact of cathodic charging on the corrosion rate of Zircaloy-4 is clearly evidenced. For the pre-hydrided samples, the impact of the cathodic treatment is expressed through higher k and n parameters in the kinetic law (0.54 and 0.38 respectively). Moreover, the greater oxidation rate of hydrided specimens is also associated with an earlier kinetic transition, both in time and thickness, with transition thicknesses close to 1.5 µm compared with 2 µm for the reference samples, as mentioned earlier.

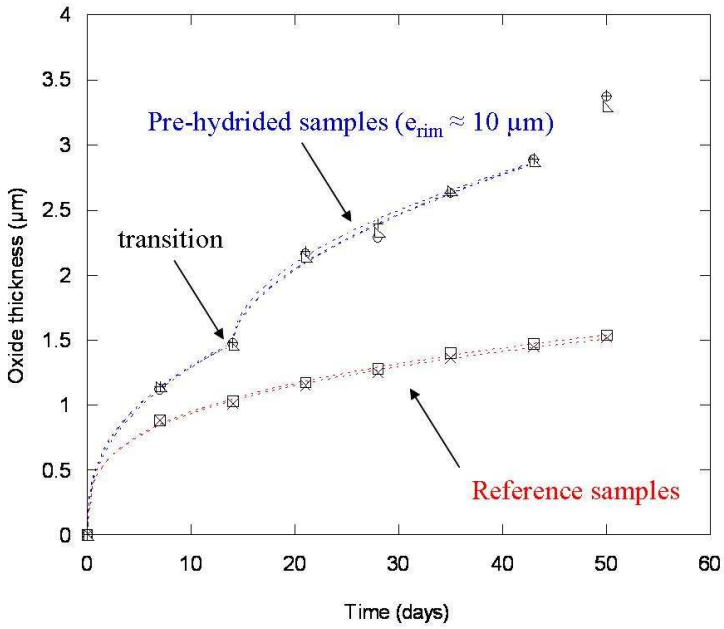

Fig. 4. Corrosion kinetics of pre-hydrided and reference Zircaloy-4 samples during corrosion in primary water at 360℃ and 18.7 MPa.

3.3 Impact of zirconium hydrides on oxide microstructure

For a same oxide thickness in the pre-transition stage, the characterization of pre-hydrided and reference samples revealed no impact of hydrides on morphology and orientation of zirconia grains in the oxide scale, as previouly observed [9]. However, on the pre-hydrided sample, a higher density of micro-cracks has been observed inside the oxide film and a new phase indexed as the sub-oxide Zr_3O located at the interface between zirconia and the massive hydride phase δ-$ZrH_{1.66}$ has been identified (figure 5).

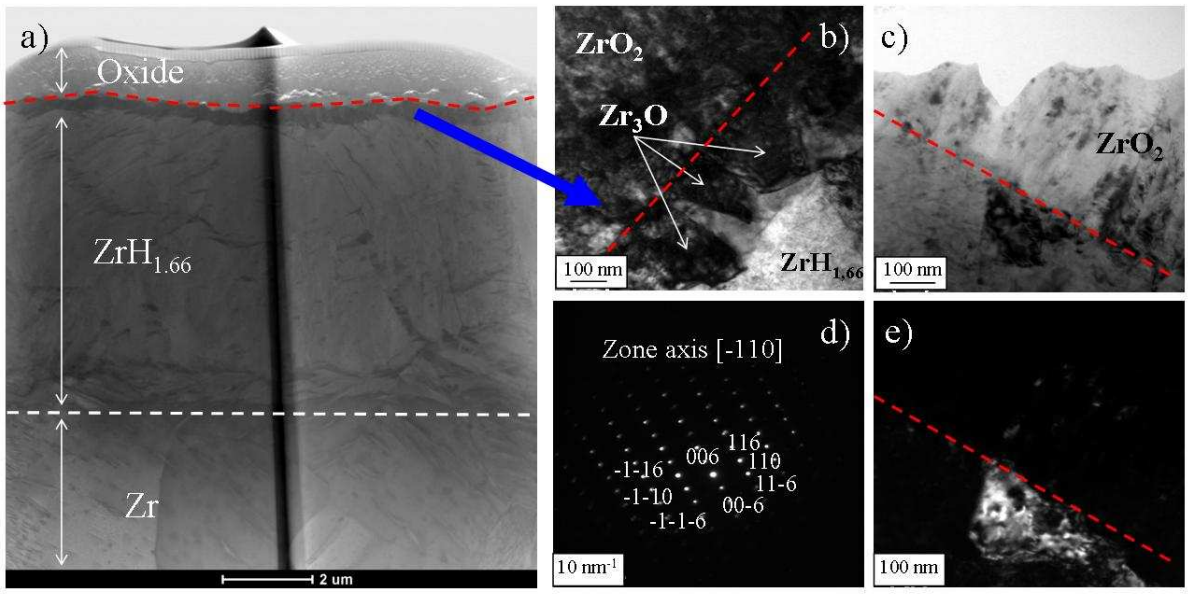

Fig. 5. (a) Micrograph in STEM mode of a pre-hydrided sample corroded 7 days at 360℃. Under the oxide region, a massive hydride phase is still present. (b) Presence of sub-oxide grains between the oxide scale and the hydride phase indexed as Zr_3O (c, d, and e) at the metal/oxide interface. Red dotted lines represent the metal/oxide interface.

To precise the impact of hydrides on the oxide microstructure, the corrosion films formed on pre-hydrided and reference samples were analysed using synchrotron microdiffraction. The local X-ray analysis allowed us to build a profile from the internal interface (metal or hydride/oxide) towards the external interface (oxide/water). The results obtained for the pre-hydrided sample corroded in primary water are presented in figure 6. Besides the major presence of the monoclinic zirconia and the δ-$ZrH_{1.66}$ hydride phase, a few diffraction picks confirmed the appearance of the sub-oxide Zr_3O and revealed the presence of a new hydride phase indexed as ε-ZrH_2 at the internal interface. Indeed, another experiment based on the corrosion in heavy primary water of pre-hydrided and reference samples pointed out, thanks to SIMS analyses, that during the corrosion process, the hydrogen initially present in the sample stays in the hydride phase and does not diffuse towards the oxide film. The accumulation of hydrogen in the vacant tetragonal sites of the δ-$ZrH_{1.66}$ phase could explain the progressive transformation into the new ε-ZrH_2 hydride phase.

Finally, a qualitative determination of the polymorphic oxide phases of zirconia, based on the empirical model proposed in [29] was carried out in order to determine the evolution of tetragonal phase through the corrosion film. In both types of samples, a higher fraction of tetragonal phase is observed near the internal interface, which confirmed previous results [30]. However, on the pre-hydrided sample, whatever the distance from the interface being considered, a lower proportion of tetragonal zirconia is always observed compared with the reference sample.

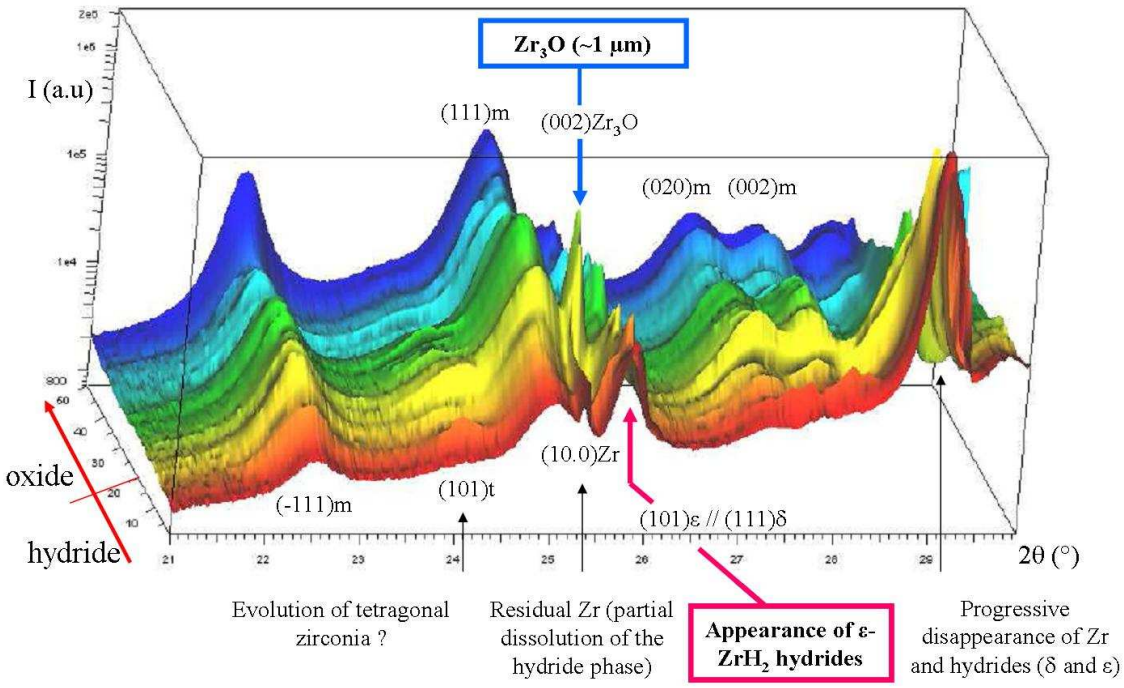

Fig 6. µ-DRX profile obtained on a pre-hydrided sample corroded in light primary water at 360℃ (oxide thickness of 7.4 µm).

3.4 Impact of zirconium hydrides on oxygen diffusion through the oxide scale

To complete this study, the impact of zirconium hydrides on oxygen diffusion through the oxide scale was investigated using the isotopic exchange with ^{18}O. The pre-transition and the post-transition phases were explored, with short and long time exposures [28] in order to compare the oxidation mechanisms between the pre-hydrided and the reference samples.
In the pre-transition stage, after the exposure of 6h and 24h in $H_2{}^{18}O$, a deeper penetration of ^{18}O is observed in the oxide scale formed on the pre-hydrided samples, leading to a twice

higher diffusion coefficient of oxygen ($2.4.10^{-15}$ cm²/s compared with $1.3.10^{-15}$ cm²/s for the reference sample, with this last result in accordance with bibliography [31]).
Moreover, in both kinetic domains (pre- and post-transition), a higher concentration of ^{18}O in the fast diffusion paths (grain boundaries, probably) can be observed on the pre-hydrided samples, as well as a faster enrichment of ^{18}O near the internal interface, which is the sign of a higher part of diffusion through the grain boundaries in corrosion films formed on hydrogen-containing samples [32]. A model based on a different structure of grain boundaries in zirconia formed on the pre-hydrided and the reference samples has been proposed [33].

4 Conclusion

Finally, the results mentioned above are useful to clarify the hydriding mechanisms of Zircaloy-4 during corrosion in reactor. Chronologically, once the hydrogen reaches the solid solution limit, zirconium hydrides precipitate in the metallic matrix and our results clearly indicate that they may impact the behaviour of Zircaloy-4 corrosion. Even if the potentiel impact of other factors proposed in literature can not be excluded, the precipitation of massive hydrides takes a real part in the appearance of the “Phase III acceleration” observed in PWRs.

5 References

[1] F. Garzarolli et al., Zirconium in the Nuclear Industry: 11th International Symposium, ASTM STP 1295, p. 12, (1996).
[2] P. Bossis et al., Zirconium in the Nuclear Industry: 14th International Symposium, ASTM STP 1467, p. 494, (2005).
[3] A. M. Garde et al., Zirconium in the Nuclear Industry: 10th International Symposium, ASTM STP 1245, 760, (1994).
[4] X. Iltis et al., Zirconium in the Nuclear Industry: 11th International Symposium, ASTM STP 1295, p. 242, (1996).
[5] P. Barberis et al., Zirconium in the Nuclear Industry: 13th International Symposium, ASTM STP 1423, p. 33, (2002).
[6] A. M. Garde, Zirconium in the Nuclear Industry: 9th International Symposium, ASTM STP 1132, p. 566, (1991).
[7] T. Kido, 6th International Symposium on Environmental Degradation of Materials in Nuclear Power Systems, p. 449, (1993).
[8] M. Blat et al., Zirconium in the Nuclear Industry: 11th International Symposium, ASTM STP 1295, p. 319, (1996).
[9] M. Blat et al., Zirconium in the Nuclear Industry: 12th International Symposium, ASTM STP 1354, p. 563, (2000).
[10] Y. S. Kim et al., Zirconium in the Nuclear Industry: 10th International Symposium, ASTM STP 1245, p. 745, (1994).
[11] Y. S. Kim et al., Zirconium in the Nuclear Industry: 13th International Symposium, ASTM STP 1423, p. 247, (2002).
[12] L. Aufore, PhD Thesis, Aix-Marseille 2 University (1997).
[13] D. Khatamian et al., Journal of Nuclear Materials, 166, p. 300, (1989).
[14] D. Khatamian, Journal of Alloys and Compounds, 253-254, p. 471, (1997).
[15] B. Cox, Journal of Nuclear Materials, 264, p. 283, (1999).
[16] E. Hillner, U.S Report, WAPD-TM-411 (1964).
[17] Ph. Bossis et al., Journal of ASTM International, 2 (2009)
[18] C. Bisor-Melloul et al., EUROCORR conference (2009)
[19] C. Wagner, Zeitschrift für Physikalische Chemie, B21, p. 25, (1933).
[20] B. Cox, Journal of Nuclear Materials, 336, p. 331, (2005).
[21] J.S. Bryner, Journal of Nuclear Materials, 82, p. 84, (1979).
[22] M. Parise et al., Journal of Nuclear Materials, 256, p. 35, (1998).
[23] B. Cox, Journal of Nuclear Materials, 29, p. 50, (1969).

[24] F. Garzarolli et al., Zirconium in the Nuclear Industry: 9th International Symposium, ASTM STP 1132, p. 395, (1991).
[25] G.P. Sabol et al., Zirconium in Nuclear Applications, ASTM STP 551, p. 435, (1974)
[26] A. Motta et al., Zirconium in the Nuclear Industry: 14th International Symposium, ASTM STP 1467, p. 205, (2005).
[27] J.J. Kearns, Journal of Nuclear Materials, 22, p. 292, (1967).
[28] C. Bisor-Melloul et al., 14th International Conference on Environmental Degradation in Nuclear Power Systems, (2009).
[29] R. C. Garvie, et al., Journal of American Ceramic Society, 55, p. 303, (1972).
[30] J. L. Béchade et al., Materials Science Forum, 404-407, p. 803, (2002).
[31] B. Cox et al., Journal of Nuclear Materials, 28, p. 73, (1968).
[32] S. Chevalier et al., Materials at High Temperature, 20, p. 253, (2003).
[33] C. Bisor-Melloul, PhD Thesis, Evry University, CEA (2010).